ELSEVIER

Catalysis Today 24 (1995) 95–101

CATALYSIS TODAY

Partial hydrogenation of 1,5,9-cyclododecatriene in three phase catalytic reactors

F. Stüber, M. Benaissa, H. Delmas *

Laboratoire de Génie Chimique-URA CNRS 192 ENSIGC-INPT, 18, Chemin de la Loge, 31078 Toulouse Cedex, France

Abstract

In this paper we report on the hydrogenation of 1,5,9-cyclododecatriene in three phase catalytic reactors with emphasis on selectivity of intermediates. Batch hydrogenations have been performed in a stirred autoclave using shell catalyst pellets and powdered pellets of 0.5% Pd on porous γ-Al_2O_3. Analysis of experimental data shows the presence of strong pore diffusion for pellets. Selectivity is found to increase slightly with temperature and with decreasing pressure. At identical operating conditions, selectivity is higher for pellets than for powder. Intrinsic kinetics are derived from complete reaction data with the powder catalyst. The model accounts for hydrocarbon adsorption as well as for pressure and temperature effects on selectivity. In the continuous packed bed reactor, gas–liquid mass transfer is strongly limiting but improves with the hydrogen flow rate. Efficiency and overall volumetric gas–liquid–solid mass transfer coefficients of the continuous reactor are calculated on the basis of experimental reaction rates of the two reactors. On the other hand, selectivity is found to be nearly unchanged due to the opposed effects of liquid back-mixing and decrease of hydrogen concentration by mass transfer limitations.

1. Introduction

Selectivity of partial hydrogenation of polyunsaturated hydrocarbons is mainly dependent on the optimal choice of the catalyst. In addition, *reaction parameters* such as pressure, temperature, concentration, catalyst particle size and *reactor hydrodynamics*, in particular gas–liquid mass transfer and residence time distribution, also define selectivity properties of consecutive reactions. These two features are investigated respectively in a batch-stirred tank reactor and in a continuous concurrent upward-flow fixed bed reactor. As a reaction of industrial interest, we have chosen the partial hydrogenation of 1,5,9-cyclododecatriene (CDT) to cyclododecene (CDE) via cyclododecadiene (CDD) avoiding complete hydrogenation to cyclododecane (CDA).

2. Kinetics in stirred batch reactors

Batch hydrogenations were performed in a stirred autoclave ($V = 500$ cm^3) at different pressures (0.15–1.2 MPa), stirrer-speeds (13–45 rps), catalyst loading and temperatures (413–453 K). Several catalyst sizes were used: alumina pellets ($D = 3$ mm, $L = 3.2$ mm) where palladium has been deposited on an external layer of 240 μm (Degussa, E 263 P/D, 0.5% Pd) and crushed pellets of mean diameter of 5, 10 and 30 μm. Experiments were run with commercially pure CDT and H_2. Liquid samples were regularly withdrawn and analysed on a HP 5890 gas chromatograph with a HP-FFAP capillary column (25 m).

* Corresponding author.

SSDI 0920-5861(95)00014-3

2.1. Mass transfer limitations

Special care was taken to measure true reaction rates in absence of physical phenomena such as pellet attrition and external mass transfer limitations.

When using *powder*, the reaction rate depended on the stirrer speed up to 35 rps under standard conditions and at maximum pressure as shown in Fig. 1. The proportionality of the reaction rate to the catalyst weight was checked in the range of 0.75 to $1.5 \cdot 10^{-3}$ kg. Independent gas–liquid mass transfer and solubility measurements have been carried out in the same equipment using the same gas and the same liquid phases. They allowed the calculation of the ratio of initial reaction rate to gas–liquid mass transfer rate in the most severe reaction conditions. This ratio was less than 0.1 confirming the absence of gas–liquid mass transfer limitations at stirrer speeds exceeding 40 rps in case of a 10 μm powder catalyst. Furthermore, equal rate constants for catalyst particle size of 5 and 10 μm indicated that the reaction occurred in the chemical regime, i.e. that no internal diffusion limitations were present during the experiments.

When using *pellets* placed as a monolayer of 10^{-2} kg in a toroidal fixed basket around the turbine, the same trend was observed as given in Fig. 1. A minimum stirrer speed of about 35 rps was required to eliminate any external mass transfer limitations. Despite this analogy, it must be emphasized that in this case, in addition to severe internal diffusion involving a much lower apparent reaction rate, *liquid–solid* mass transfer is the limiting external step. Indeed, the hydrogen consumption rate being much reduced for pellets, a lower stirrer speed would be required to achieve the corresponding gas–liquid transfer, as far as the catalyst monolayer did not considerably alter $K_l a$. On the contrary, for large pellets the external particle area and thus the liquid–solid mass transfer were strongly reduced. At stirrer speeds above 40 rps, attrition became significant and this data were not considered in the kinetic analysis.

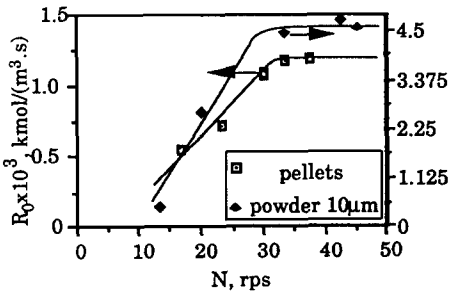

Fig. 1. Influence of agitation speed on initial reaction rate. $C_{CDTO} = 5.012$ kmol m^{-3}, $T = 433$ K, $m_{cat} = 0.75$ g and $PH_2 = 0.6$ MPa (powder); $T = 443$ K, $m_{cat} = 10$ g and $PH_2 = 1.2$ MPa (pellets).

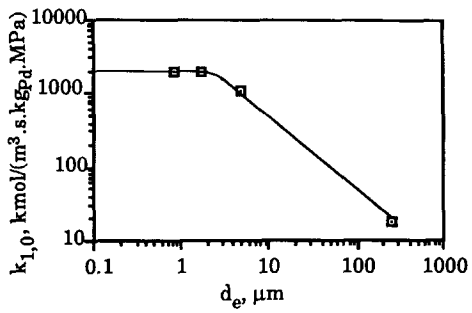

Fig. 2. Initial rate constants as function of catalyst equivalent particle diameter. $T = 433$ K, $C_{CDTO} = 5.012$ kmol m^{-3} ($d_e = d_p/6$ for powder and $d_e = 240$ μm for pellets 3×3.2 mm).

The results for different particle sizes of catalyst are compared in Fig. 2. Equal rate constants were observed for 5 and 10 microns while the value of the pellets was found to be considerably lower. From the experimental data the effectiveness factor of the pellets was evaluated to be about 0.01. The effective diffusivity was then calculated according to the apparent module of Weisz:

$$D_{eff} = \frac{R_0 \cdot L^2}{\phi_s \cdot C^*_{H_2}} = 2.45 \cdot 10^{-9} \text{ m}^2/\text{s} \qquad (1)$$

Using a convenient correlation for the molecular diffusivity [1], the tortuosity [$\tau = D\epsilon/D_{eff}$] was estimated to be 7.2. Arrhenius law was checked for both fine powder and pellets and the respective activation energies were determined: $E = 40$ kJ/mol and $E_{ap} = 26$ kJ/mol. This result confirms the well known effect of pore diffusion, expressed as $E_{ap} = (E + E_D)/2$. The moderate true activation energy is in good agreement with that observed for many other hydrogenations.

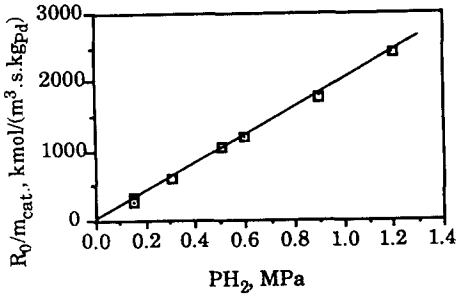

Fig. 3. Influence of pressure on the initial reaction rate per unit catalyst weight. $T=433$ K and $C_{CDT0}=5.012$ kmol m^{-3}.

2.2. Intrinsic kinetics and selectivity

The initial reaction rate per unit catalyst weight was of the first order with respect to hydrogen as plotted in Fig. 3. This suggests that, in the pressure range of 0.15 to 1.2 MPa studied and for high hydrocarbon concentrations, hydrogen adsorption has negligible effects on site coverage and may be disregarded in the kinetic equation.

Concerning the complete reaction, a large set of experimental data, relative to the four species involved in the reaction scheme, was obtained as illustrated in Fig. 4. The concentration–time profiles do not distinguish between the various isomers (6 for CDT, 6 for CDD and 2 for CDE) detected by chromatography. Unlike the kinetic study of Hanika et al. [2], isomerization of CDT clearly took place at elevated temperatures. The maximum fraction of the main isomer reached about 15% of initial CDT. Although different reaction rates of these isomers are probable from a chemical point of view, a complete lumping of the isomers was yet necessary for kinetic parameter optimization.

For industrial purpose, maximum yields of CDE were required and selectivity, being then the major challenge, has to be discussed. The two intermediates, CDD and CDE, exhibit a classical optimum as seen in Fig. 4. The maxima of CDD are roughly constant at 55% while the desired maxima of CDE are significantly improved with decreasing hydrogen pressure. Similar behaviour was found by McAlister et al. [3], Barinov et al. [4,5] and for homogeneous catalytic hydrogenation of CDT by Fahay [6]. Such pressure effect on the selectivity of consecutive hydrogenations has also been observed in several cases but very

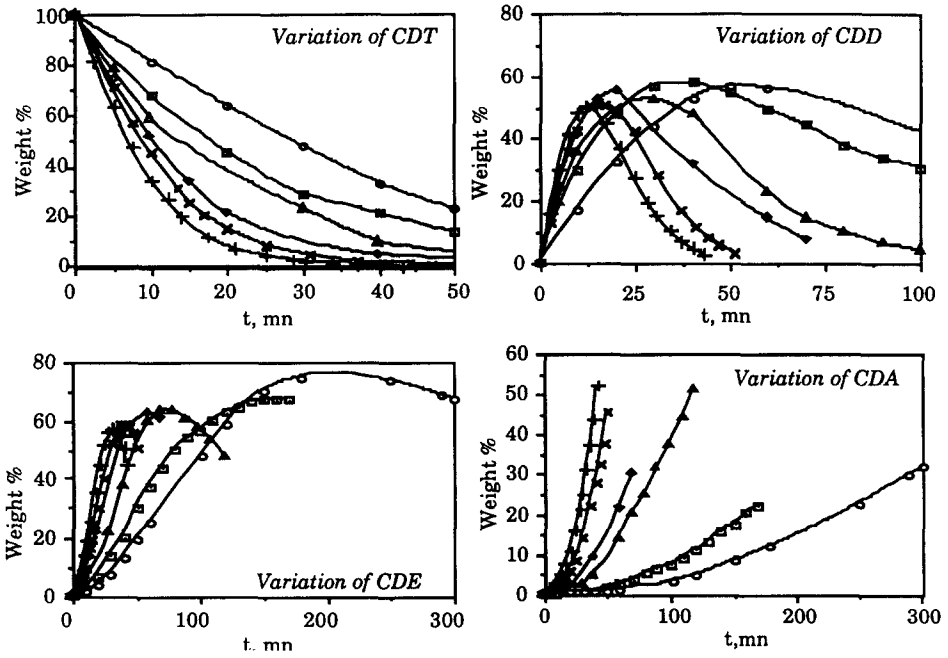

Fig. 4. Influence of pressure on the variation of hydrocarbon weight fractions. $T=433$ K, $C_{CDT0}=5.012$ kmol m^{-3} and $m_{cat}=0.75$ g. ○, 0.15 MPa; △, 0.5 MPa; ×, 0.9 MPa; □, 0.3 MPa; ◇, 0.6 MPa; +, 1.2 MPa.

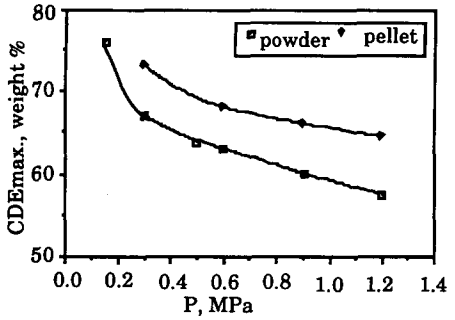

Fig. 5. Influence of pressure on the maximum of CDE; effect of particle size. $T=433$ K and $C_{CDT0}=5.012$ kmol m^{-3}.

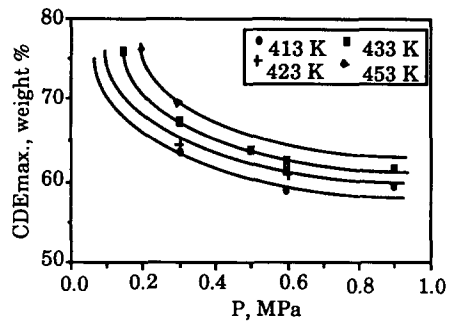

Fig. 6. Influence of pressure and temperature on the maximum of CDE, with powder catalyst.

different explanations have been proposed [7].

Selectivity is also higher with pellets than with powder as shown in Fig. 5. This unusual effect can be understood by a decrease in the effective hydrogen concentration at the catalytic surface due to pore diffusion. On the other hand, selectivity is increased with rising temperature as reported in Fig. 6 and also observed earlier [3–6]. The temperature effect was supposed to be a result of different activation energies rather than of different heats of adsorption.

A simplified kinetic modelling was tested using complete reaction data of 5 and 10 μm powder in the pressure and temperature range studied. The three hydrogenations have the following intrinsic rate equations:

$$R_i=\frac{m_{Pd}k_iK_jC_jP_{H_2}^{\alpha}}{(1+K_{CDT}C_{CDT}+K_{CDD}C_{CDD}+K_{CDE}C_{CDE})},$$

$$i=1,\ 2 \text{ and } 3;\ j=\text{CDT, CDD and CDE} \quad (2)$$

The Arrhenius law defines the rate constants k_i and adsorption constants K_j as: $k_i=k_{i,0}e^{-Ei/RT}$ and $K_j=K_{j,0}e^{-Aj/RT}$. In order to minimize the number of kinetic parameters to be simultaneously optimized, the activation energy and heat of adsorption of the first order hydrogenation of CDT to CDD have been derived from initial kinetics. The three heats of adsorption were supposed to be equal and only the activation energy of the last hydrogenation step was optimized. The results of the optimization procedure are summarized in Table 1.

The exponent of hydrogen pressure in the second hydrogenation step was found to be very close to 1. On the contrary, the effect of pressure on selectivity was accounted for by an exponent of 1.36 in the last hydrogenation. In fact, the kinetic model does not explain the chemical features of the observed selectivity effects. However, a good fit was obtained for the experimental range and especially for the optimum of CDE as demonstrated by the example in Fig. 7.

3. Continuous reaction in fixed bed upflow reactor

Two types of continuous reactors, bubble column slurry reactors and fixed bed downflow reactors (trickle beds), are generally used to carry out three phase reactions. However, in the case of

Table 1
Kinetic parameters for L–H model

Frequency factor (kmol/(m^3 s MPa$^{\alpha}$ kg cat.)	Activation energy (kJ/kmol)	Frequency factor for adsorption (m^3/kmol)	Heat of adsorption (kJ/kmol)
$k_{1,0}=14.22\cdot10^7$, $\alpha=1.0$	$E_1=40\cdot10^3$	$K_{CDT,0}=38.36$	$A_{CDT,0}=14\cdot10^3$
$k_{2,0}=16.42\cdot10^7$, $\alpha=1.0$	$E_2=40\cdot10^3$	$K_{CDD,0}=15.74$	$A_{CDD,0}=14\cdot10^3$
$k_{3,0}=7.89\cdot10^7$, $\alpha=1.36$	$E_3=35\cdot10^3$	$K_{CDE,0}=10.0$	$A_{CDE,0}=14\cdot10^3$

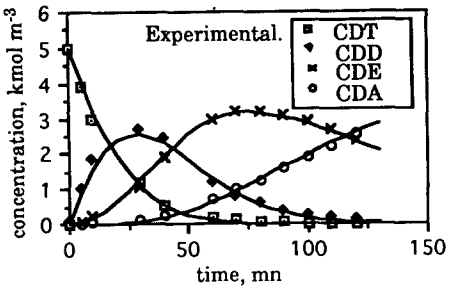

Fig. 7. Experimental concentration data for catalyst powder and model predictions. $T=433$ K, $PH_2=0.5$ MPa, $C_{CDTO}=5.012$ kmol m^{-3} and $m_{cat}=0.75$ g.

Table 2
Experimental conditions

	1. Stage	2. Stage
Operating data		
Cooling temperature (K)	423–438	443–463
Reactor pressure (MPa)	0.2–0.6	0.15–0.25
Liq. flow rate (10^{-7} m^3/s)	2.9–5.5	5–6
Gas flow rate (10^{-4} m^3/s)	0.9–3.25	0.4–0.9
Reactor data		
(D_i/D_a) reactor (m)	$(2.6/2.9)\cdot10^{-2}$	
(D_i/D_a) jacket (m)	$(4/5)\cdot10^{-2}$	
Height of reactor (m)	1.5	
Bed porosity	0.36	
Bed weight (kg)	0.71–0.73	
Bed density (kg/m^3)	800–830	

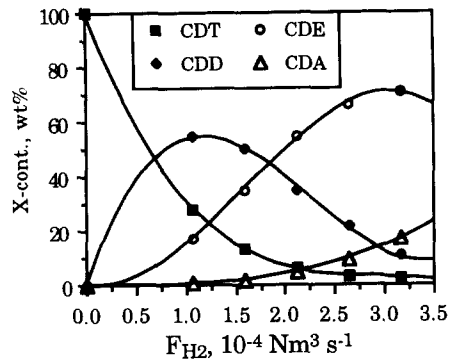

Fig. 8. Outlet concentration of hydrocarbons vs. hydrogen flow rate in continuous reactor: $PH_2=0.6$ MPa, $T_{cool.}=423$ K, $F_{liq.}=5.5\cdot10^{-7}$ m^3 s^{-1}, $t_{res.}=5$ min, $m_{cat}=0.715$ kg.

consecutive hydrogenation reactions, where the constraints of selectivity and exothermicity are combined, the use of a fixed bed reactor with concurrent upflow mode and proper temperature control promises better reactor performance.

Thus, the selective hydrogenation was investigated in a pilot scale upflow mode reactor packed with the same cylindrical catalyst pellets as used in the stirred autoclave. The bed, 1.5 m in height, was equipped with 4 thermocouples and 4 liquid sample valves to measure axial profiles. Temperature control was achieved by means of a cooling oil circulating in a jacket. The experiments were performed under steady state conditions of reaction. Steady state conditions corresponded simultaneously to stable axial reactor temperatures and constant concentrations at the reactor outlet. At given liquid flow rate, pressure and marlotherm temperature, the hydrogen flow rate was increased step by step and the concentration changes were measured at the reactor outlet.

Preliminary runs defined a suitable operating range, especially concerning thermal stability which was mainly affected by three parameters: the two flow rates and the marlotherm temperature. When increasing the liquid flow rate with hydrogen fed in a stoichiometric ratio, an increasing maximum temperature, up to 463 K, was observed in the bed. This was the limit of stable thermal behaviour. At higher liquid flow rates temperature runaway occurred in the bed regardless to the chosen cooling temperature. Operating conditions and reactor characteristics are summarized in Table 2.

Fig. 8 shows a typical plot of the hydrocarbon fractions at the reactor outlet ($X_{cont.}$) as a function of the hydrogen flow rate. As the hydrogen flow rate was increased, the conversion of CDT tended towards completion and CDD as well as CDE passed through maxima. The actual reaction rate was thus enhanced due to higher gas–liquid mass transfer which is known to strongly depend on the gas flow rate. These concentration variations versus the hydrogen flow rate are very similar to the concentration time profiles obtained in the batch reactor as seen in Fig. 9. To examine closely this analogy, the comparison was made for similar operating conditions, i.e. same pressure and temperature.

In both reactors the maximum values of CDD and CDE are close and the peaks occurred for the

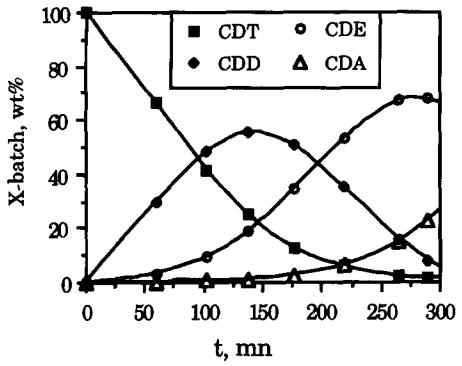

Fig. 9. Time–concentration profile of hydrocarbons in batch reactor: $PH_2 = 0.6$ MPa, $T_r = 433$ K, $V_{agitation} = 35$ rps, $m_{cat} = 0.01$ kg.

CDD at the intersection of CDT and CDE and for the CDE somewhat after the intersection of CDD and CDA as shown in Fig. 9. The comparison at the optimum of CDE is possible for both activity and selectivity because the concentration fractions are similar in the two reactors. Thus, the overall conversion is nearly the same, about 2/3 of complete hydrogenation. The average consumption rate of hydrogen per unit catalyst weight $R^*_{H_2}$ (kmol H_2/s/kg Pd), based on the true residence time of the liquid phase (accounting for the liquid hold up), is clearly lower in the packed bed. It amounts to only 44% of that of the well-mixed batch reactor. This ratio is also a measure of the overall external limitations of gas–liquid as well as liquid–solid mass transfer. This means that the equivalent pressure at the pellet surface is only 0.27 MPa corresponding to a batch maximum of CDE of 74%, i.e. 3% more than actually obtained in continuous operation. The selectivity loss at equal equivalent pressure is certainly caused by liquid mixing in the fixed bed. In the present case, it is somewhat lower than the selectivity gain due to pore diffusion, but it should substantially increase at lower liquid flow rates.

The extended comparison of both reactor performances is illustrated in Fig. 10 in terms of packed bed efficiency $\eta^*(R^*_{H_2}/R^*_{H_2,pellet})$ calculated for different hydrogen velocities and corresponding conversion. The effect of liquid back-mixing in a packed bubble column reactor will alter selectivity but not the overall rate as long as very high conversions are not reached. Then, the reactor efficiency η^* can be used to calculate an overall volumetric gas–liquid–solid mass transfer coefficient $K_{ls}a$, assuming plug flow:

$$K_{ls}a = R_{H_2}/C_{H_2,equil.}/(1-\eta^*),$$

$$\text{where } R_{H_2} = F_l(X_D + 2X_E + 3X_A)/V_R \qquad (3)$$

R_{H_2} (kmol $H_2/m^3/s$) is the overall consumption rate of hydrogen calculated at each conversion, V_R (m^3) the reactor volume and F_l (kmol/s) the molar liquid flow rate. $K_{ls}a$ variations with hydrogen velocity are plotted in Fig. 10. These results are only rough estimates. However, as derived from reaction runs, they are more reliable than data from the numerous correlations of the literature obtained for different conditions and especially for different liquids.

To conclude, concerning the design of multiphase reactor for selective reactions, the packed

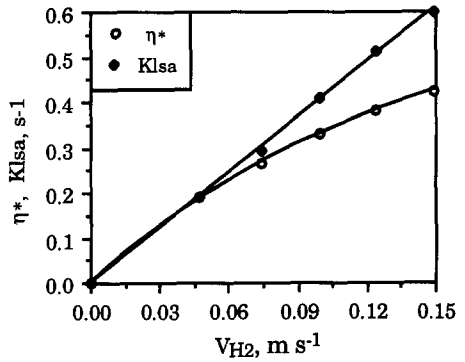

Fig. 10. Variation of reactor efficiency η and $K_{ls}a$ with respect to hydrogen velocity (same operating conditions as in Figs. 8 and 9).

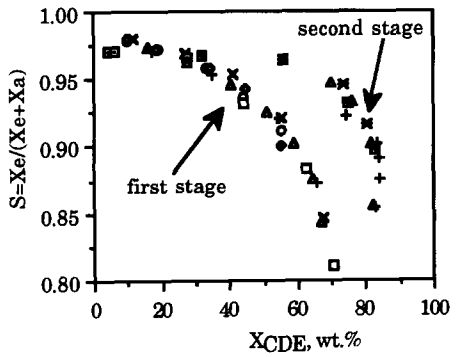

Fig. 11. Selectivity of continuous staged reactor as a function of CDE fraction (operating conditions listed in Table 2).

bed bubble column reactor performs fairly well due to efficient heat transfer as well as reduction and control of dissolved hydrogen by pore diffusion and gas flow rate respectively. To minimize the negative effect of axial mixing on selectivity, sufficiently high liquid-flow rates are required. This leads to higher reactor length to reach maximum concentration of CDE. Higher reactor length was simulated by splitting up the process in two stages resulting in a significant improvement of selectivity as shown in Fig. 11. In a commercial plant, in order to combine high selectivity and reasonable reactor length, hydrogen must be fed at stoichiometric ratio corresponding to complete conversion to CDE. In these conditions, low gas flow rate, and hence low mass transfer and low dissolved hydrogen are achieved in the last reaction zone, leading to high selectivity. The reactor can also be staged, with lower pressure but higher temperature in the last stages where no runaway can occur. In this way, high yields of CDE, up to 90%, were attained in 5 reactor stages.

References

[1] M. Diaz, A. Vega and J. Coca, Chem. Eng. Comm., 52 (1987) 271.
[2] J. Hanika, I. Svoboda and V. Ruzicka, Coll. Czech. Chem. Commun., 46 (1981) 1039.
[3] C.G. McAlister and L. Charles, U.S. Patent No. 3 400 164 (1968).
[4] N.S. Barinov, D.V. Mushenko and Y.V. Blandin, Zh. Prikl. Khim. (translated), 47 (4) (1974) 900.
[5] N.S. Barinove, I.A. Makarovskii, D.V. Mushenko and Y.V. Blandin, Zh. Prikl. Khim. (translated), 47 (12) (1974) 2711.
[6] D.R. Fahay, J. Org. Chem., 38 (1) (1973) 80.
[7] C. Niklasson, B. Andersson and N.-H. Schöön, Ind. Eng. Chem. Res. 26 (1987) 1459.